Organic solar cell performance of BODIPY and coumarin functionalized SWCNT or graphene oxide nanomaterials

Ahmet Şenocak[a], Esra Nur Kaya[a], Burak Kadem[b], Tamara Basova[c,d], Erhan Demirbaş[a], Aseel Hassan[e] and Mahmut Durmuş[a]*

[a.] Gebze Technical University, Department of Chemistry, Gebze, Kocaeli 41400, Turkey
[b.] Department of Physics, College of Science, University of Babylon, Iraq
[c.] Nikolaev Institutes of Inorganic Chemistry SB RAS, Lavrentiev Pr. 3, Novosibirsk 630090, Russia
[d.] Novosibirsk State University, Pirogova Str. 2, Russia
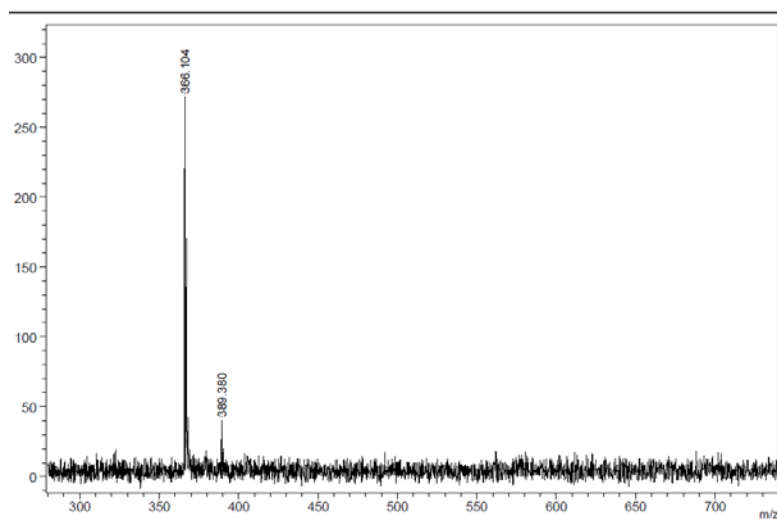[e.] Material and Engineering Research Institute, Sheffield Hallam University, UK

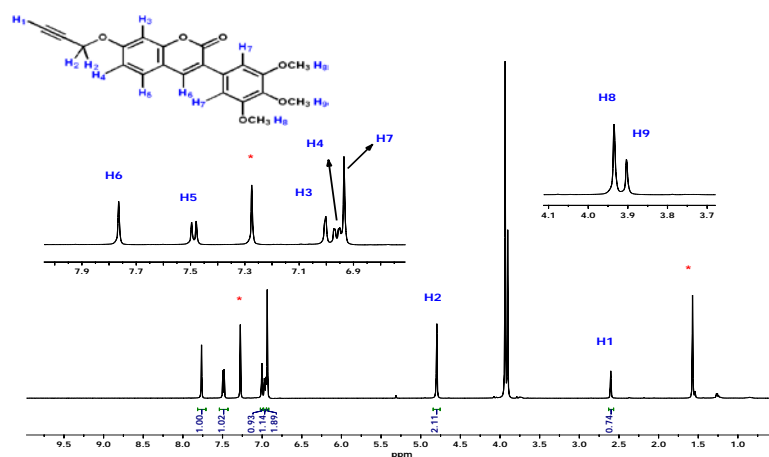Fig. S1. MALDI-TOF mass spectrum of the compound 4
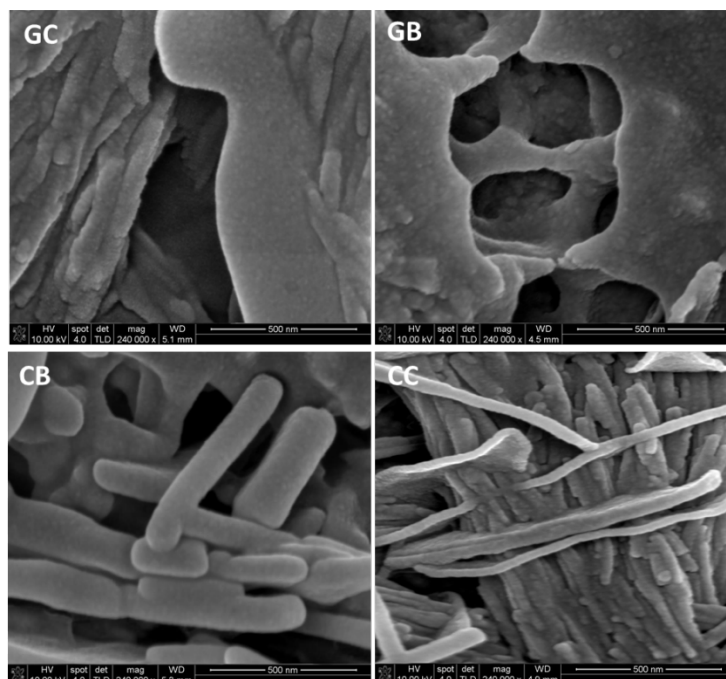

Fig. S2. ^{1}H-NMR spectra of the compound 4

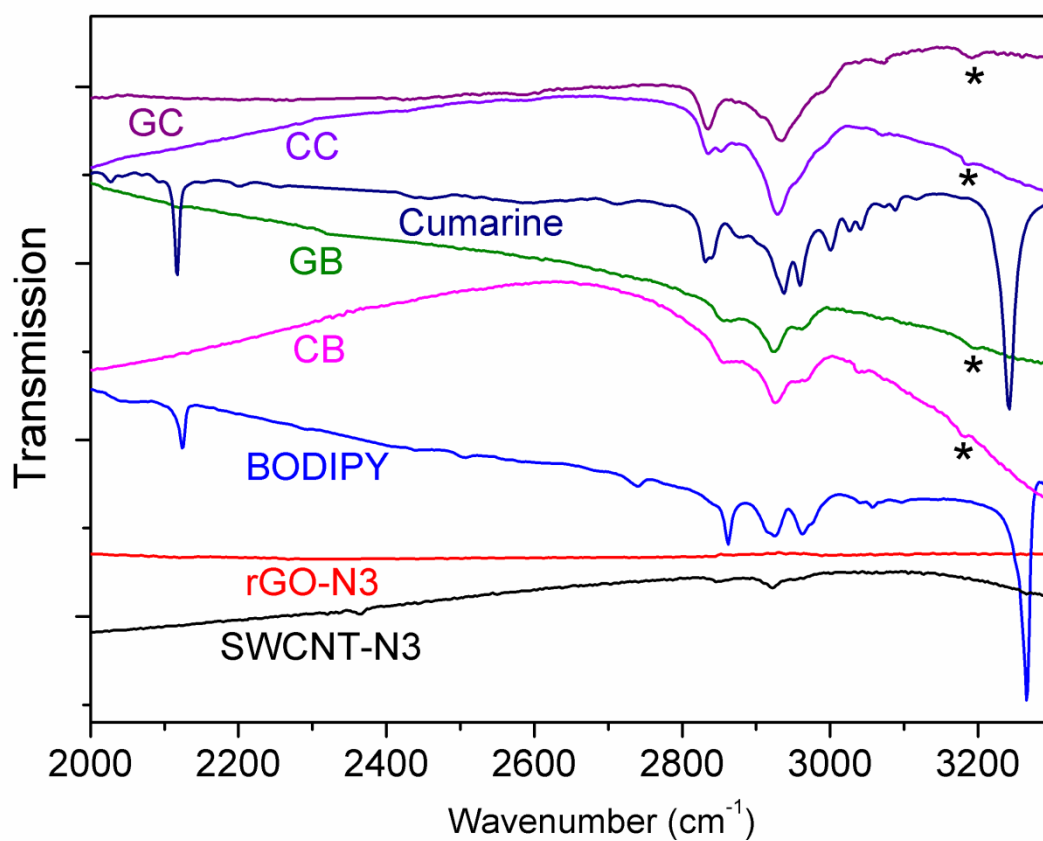Fig. S3. SEM images of the investigated hybrids.

Fig. S4. FTIR spectra of SWCNTs-N3, rGO-N3, pristine BODIPY, pristine coumarin and their CB, GB, CC and GC hybrids. The vibration peaks corresponding to CH stretchings in triazole rings are marked with asterisks (*).
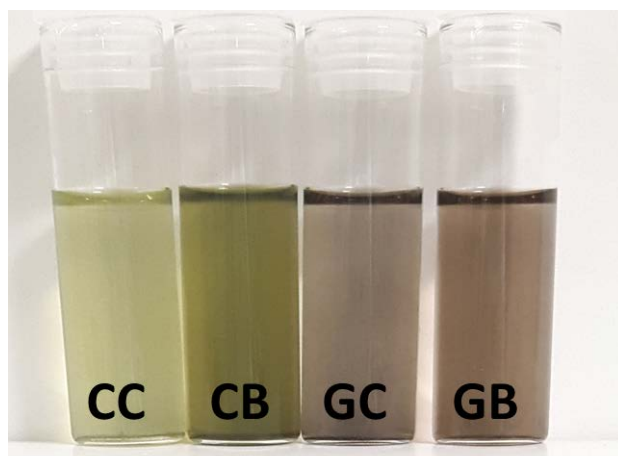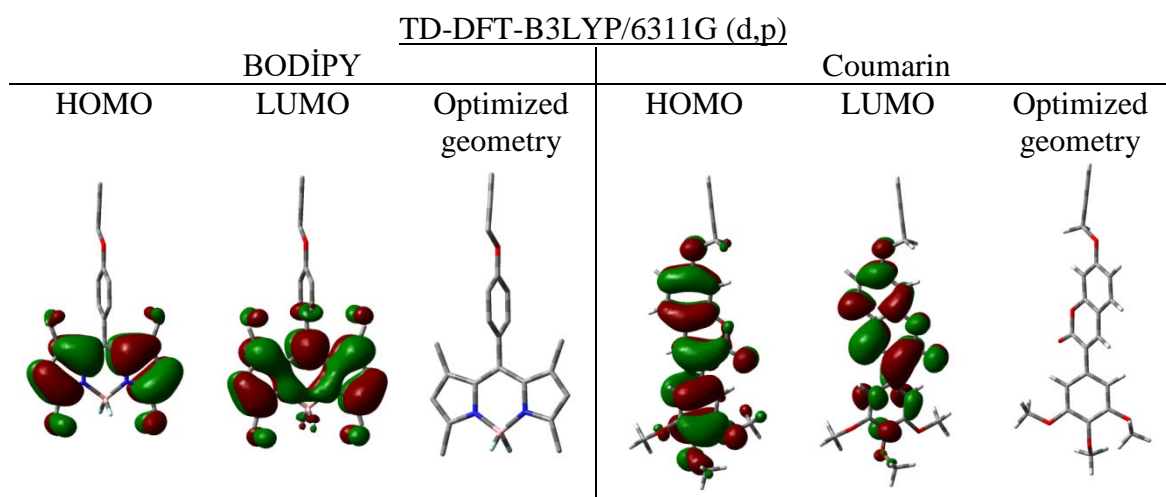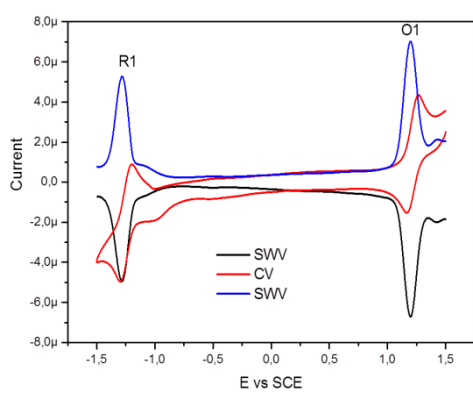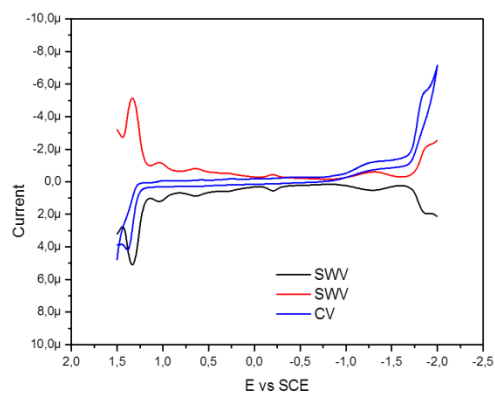
Fig. S5. Hybrid suspended in DMF.

TD-DFT-B3LYP/6311G (d,p)

BODİPY			Coumarin		
HOMO	LUMO	Optimized geometry	HOMO	LUMO	Optimized geometry

Figure S6. HOMO-LUMO orbitals and optimized geometry of of BODIPY and cumarin

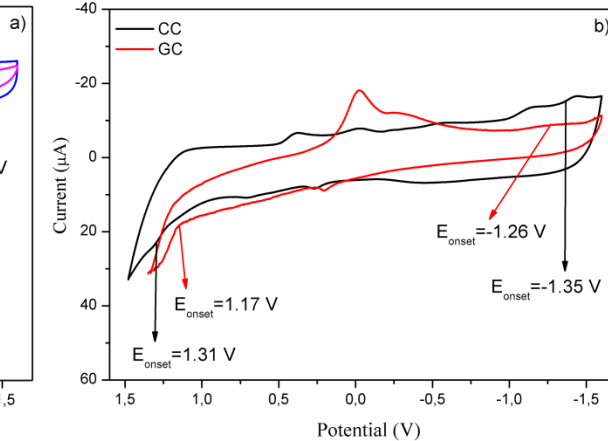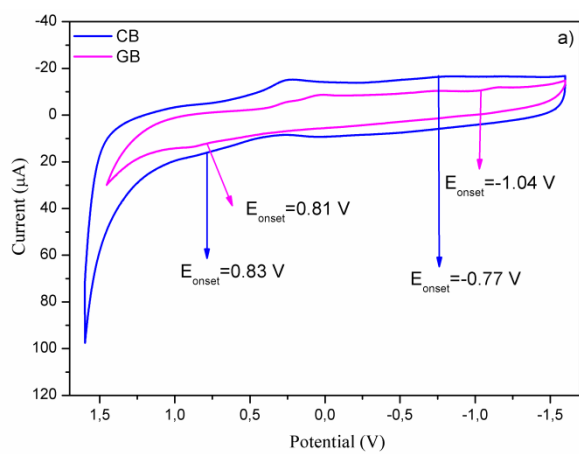Figure S7. Cyclic and square wave voltammogram of BODIPY (a) and cumarin (b)

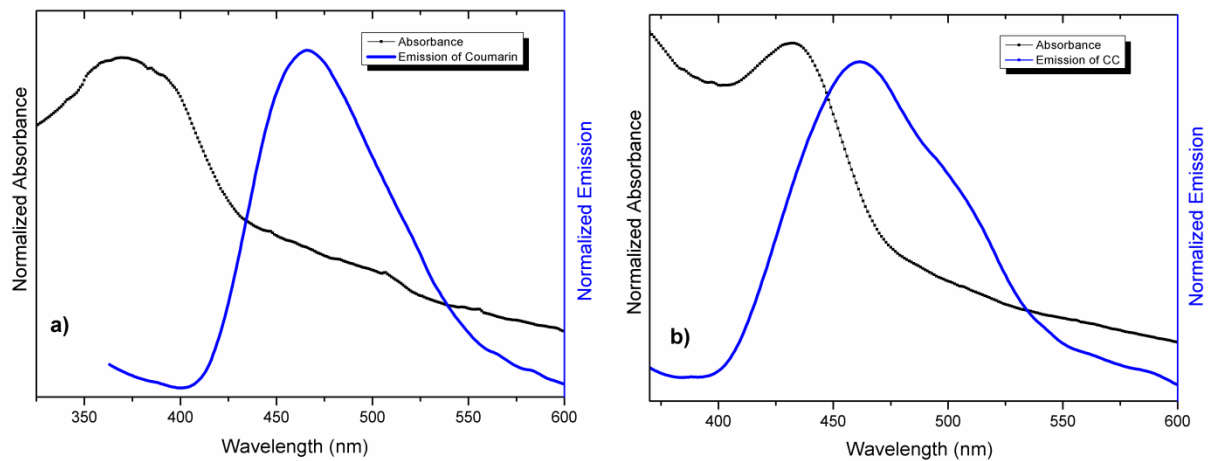Figure S8. Cyclic voltammogram of CB, GB (a) and CC, GC (b)

Figure S9. Thin film absorbance and emission spectra of the coumarin and CC.

Table S1: The HOMO and LUMO energy levels and the energy band gap (eV) of the BODIPY, coumarin and hybrids determined from cyclic voltammetry, optical absorption spectra and DFT methods

	Coumarin	BODIPY	CC	GC	CB	GB
E_{ox}	1.22	1.15	1.31	1.17	0.81	0.83
E_{red}	-1.71	-1.17	-1.35	-1.26	-1.04	-0.77
E_{HOMO}	-5.95	-5.88	-6.04	-5.90	-5.54	-5.56
E_{LUMO}	-3.02	-3.56	-3.38	-3.47	-3.69	-3.96
E_g (cyclic)	2.93	2.32	2.66	2.43	1.85	1.60
E_g (optical)*	2.85	2.44	2.77	2.80	2.39	2.37
E_g (DFT)	3.39	2.89	-	-	-	-

*Optical E_g values were estimated using the intersection points of absorption and emission spectra in thin films as shown in Fig. S9.